Electronic Supplementary Material (ESI) for Physical Chemistry Chemical Physics.

Supporting Information for

How Active Sites Facilitate Charge-transfer Interactions of Silver and Gold Clusters with TCNQ?

Jing Chen, Zhixun Luo, and Jiannian Yao**

State Key Laboratory for Structural Chemistry of Unstable and Stable Species, and Key Laboratory of Photochemistry, Institute of Chemistry, Chinese Academy of Sciences, Beijing, 100190, China.

**E-mail: zxluo@iccas.ac.cn; jnyao@iccas.ac.cn*

This part includes:

(1) Choice of methods (Tables S1-2);

(2) Structures of Ag_{13}/Au_{13}/Au_1Ag_{12}/$Au_{12}Ag_1$ clusters (Figures S1-3);

(3) Fukui functions of 13-atom clusters and TCNQ (Figures S4-5);

(4) Natural bond orbital (NBO) charge on Ag_{13} and Au_{13};

(5) Spin density of Ag_{13}/Au_1Ag_{12}/Au_{13}/$Au_{12}Ag_1$-TCNQ complexes (Figures S6-7);

(6) Natural charge distribution in Ag_{13}/Au_{13}/Au_1Ag_{12}/$Au_{12}Ag_1$-TCNQ complexes (Figures S8-9).

Table S1 Ionization energy (IP), HOMOs, and Electron affinity of neutral edge-site adsorbing Au_{13}-TCNQ, and HOMOs of anion of edge-site adsorbing Au_{13}-TCNQ.

	Ionization energy(eV)	HOMO (neutral) (eV)	Electron affinity (eV)	HOMOs(anion) (eV)
PBE0/Lanl2dz(tzp)	6.930	-6.243	3.341	-2.720
PBE0/def2-tzvp	6.923	-6.219	3.298	-2.702
LC-wPBE/def2-tzvp	7.362	-7.967	2.856	-3.788
M06-2X/def2-tzvp	7.111	-6.857	3.124	-2.890

Table S2 Ionization energy (IP), HOMOs, and Electron affinity of neutral edge-site adsorbing Au_{13}-TCNQ, and HOMOs of anion of edge-site adsorbing Ag_{13}-TCNQ.

	Ionization energy(eV)	HOMO (neutral) (eV)	Electron affinity (eV)	HOMOs(anion) (eV)
PBE0/Lanl2dz(tzp)	5.391	-6.297	2.877	-2.364
PBE0/def2-tzvp	6.351	-5.464	2.925	-2.413
LC-wPBE/def2-tzvp	6.914	-6.840	2.298	-3.331
M06-2X/def2-tzvp	6.514	-5.854	2.691	-2.718

Considering that PBE0 and LC-wPBE functionals lead to relatively large differences between electron affinity (EA) and –HOMO(anion) of 13-atom metal-TCNQ complexes (Tables S1-S2), we emphasize the results calculated at M06-2X/def2-tzvp level of theory.

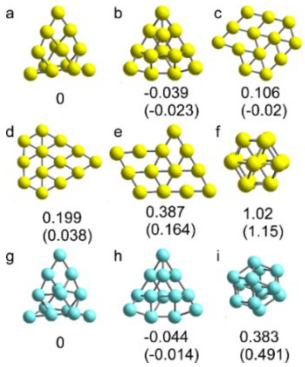

Figure S1. Local minima of Au_{13} (a-f) and Ag_{13} (g-i) optimized at PBE0/LANL2DZ level of theory. Energies calculated at PBE0/LANL2DZ and BP86/LANL2DZ (in the parentheses) level of theory relative to bilayer atomic structured Au_{13} (a) and Ag_{13} (g) are given at the bottom of each isomer, respectively.

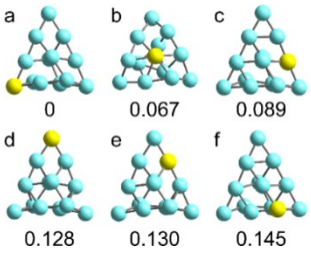

Figure S2. Structures of the $Ag_{12}Au_1$ clusters at each sites (a-f) optimized at PBE0/LANL2DZ level of theory. The relative energies with respect to corner-substitution isomer are given at the bottom of each $Ag_{12}Au_1$ isomers (in eV).

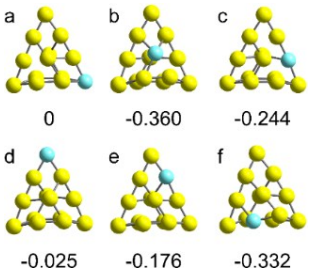

Figure S3. Structures of the Ag_1Au_{12} clusters at each sites (a-f) optimized at PBE0/LANL2DZ level of theory. The relative energies with respect to corner-substitution isomer are given at the bottom of each Ag_1Au_{12} isomers (in eV).

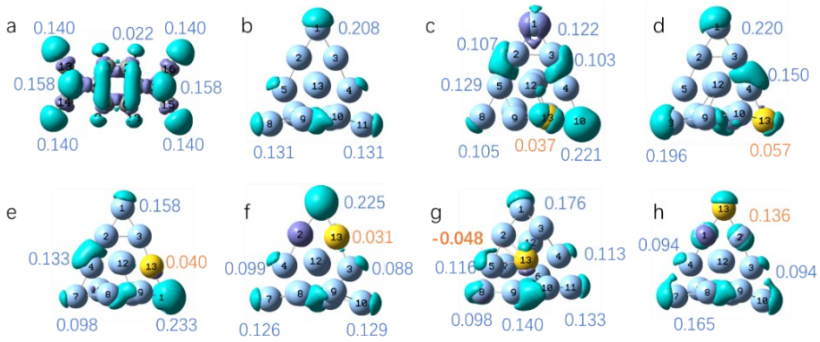

Figure S4. Isosurfaces of the acceptor, f^+, Fukui function (a) and the donor, f^-, Fukui functions (b-h) of Ag_{13} and Au_1Ag_{12} as the density differences. (a) TCNQ, (b) Ag_{13}, (c-h) Au_1Ag_{12} with Au atom at bottom (c), corner (d), edge2 (e), edge (f), face (g), and tip (h) sites, calculated at M06-2X/def2-tzvp level of theory. The values of Fukui functions of donor f^- at electrophilic and nucleophilic regions are given aside. The values of f^- Fukui functions at Au atom is given in orange text.

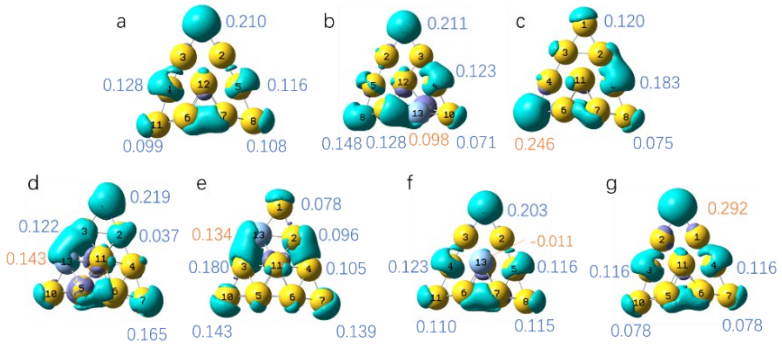

Figure S5. Isosurfaces of the donor, f^-, Fukui functions of Au_{13} (a) and $Au_{12}Ag_1$ (b-g) as the density differences. (b-g) $Au_{12}Ag_1$ with Au atom at bottom (b), corner (c), edge2 (d), edge (e), face (f), and tip (g) sites, calculated at M06-2X/def2-tzvp level of theory. The values of Fukui functions of donor f^- at nucleophilic regions are given aside. The values of f^- Fukui functions at Ag atom is given in orange text.

Table S3. NBO charge on Ag_{13} and Au_{13} clusters and binding energy between metal cluster and TCNQ in the edge-site adsorbing complexes calculated at M06-2X/def2-tzvp level of theory.

Substitution sites	Bottom	Edge	Face	Tip
Charge on Ag_{13}	0.759	0.797	0.725	0.742
BE (Ag_{13}-TCNQ)	1.913	1.496	2.043	2.496
Charge on Au_{13}	0.664	0.680	0.120	0.240
BE (Au_{13}-TCNQ)	1.166	1.193	0.666	0.268

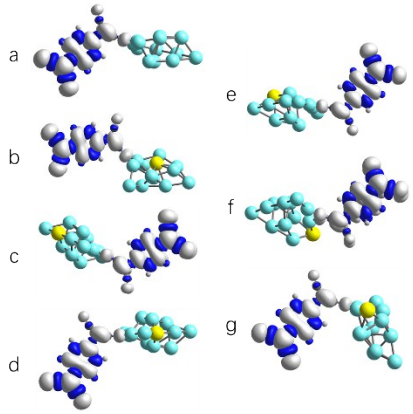

Figure S6. Spin density of Ag_{13}/Au_1Ag_{12}-TCNQ complexes calculated at M06-2X/def2-tzvp level of theory. (a) Ag_{13}-TCNQ, (b-g) Au_1Ag_{12}-TCNQ with Au substitution at (b) face, (c) edge2, (d) edge, (e) bottom, (f) corner, and (g) tip sites.

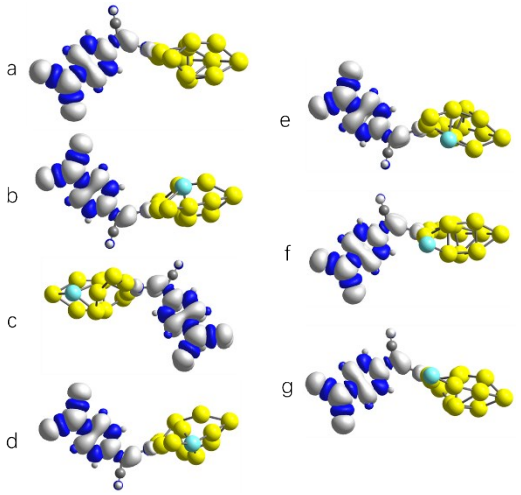

Figure S7. Spin density of Au_{13}/$Au_{12}Ag_1$-TCNQ complexes calculated at M06-2X/def2-tzvp level of theory. (a) Au_{13}-TCNQ, (b-g) $Au_{12}Ag_1$-TCNQ with Au substitution at (b) face, (c) edge2, (d) edge, (e) bottom, (f) corner, and (g) tip sites.

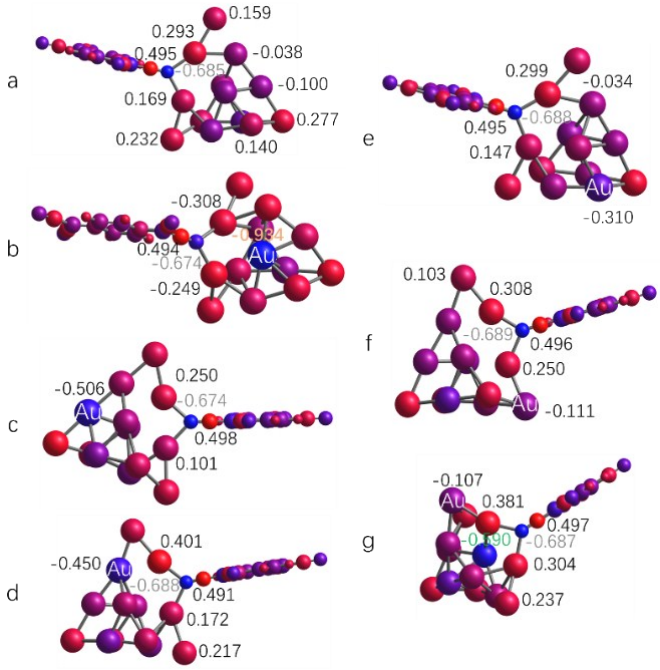

Figure S8. NBO charge on N, C, and Au atoms in Ag_{13}/Au_1Ag_{12}-TCNQ complexes calculated at M06-2X/def2-tzvp level of theory. (a) Ag_{13}-TCNQ, (b-g) Au_1Ag_{12}-TCNQ with Au substitution at (b) face, (c) edge2, (d) edge, (e) bottom, (f) corner, and (g) tip sites.

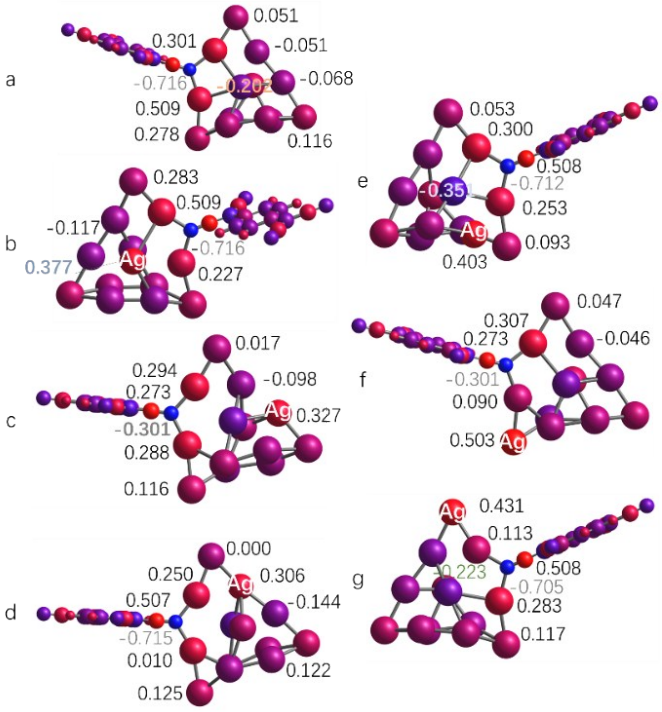

Figure S9. NBO charge on N, C, and Ag atoms in Au_{13}/$Au_{12}Ag_1$-TCNQ complexes calculated at M06-2X/def2-tzvp level of theory. (a) Au_{13}-TCNQ, (b-g) $Au_{12}Ag_1$-TCNQ with Ag substitution at (b) face, (c) edge2, (d) edge, (e) bottom, (f) corner, and (g) tip sites.